Improving a Scallop Dredge Bag to Reduce Fish Bycatch Using Flume Tank Testing and Computational Fluid Dynamics

Final Report

Prepared for the 2017
NOAA Scallop research Set-Aside
(Grant # NA17NMF4540036)
May 2018

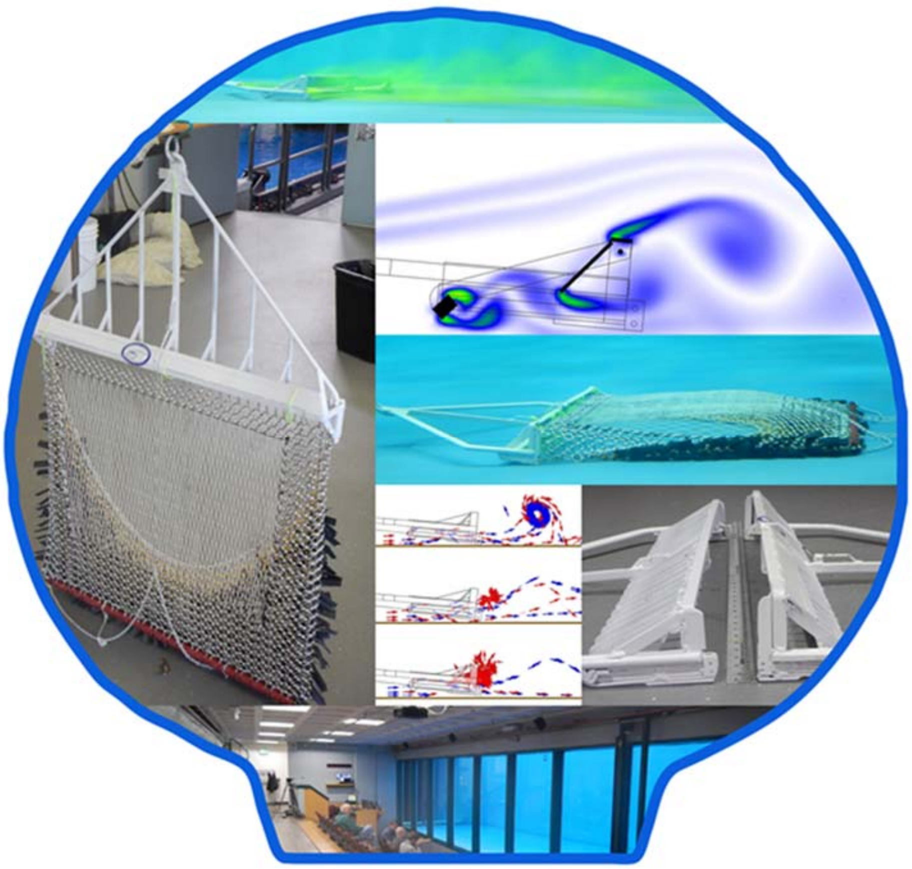

Submitted By

Liese Siemann and Farrell Davis
Coonamessett Farm Foundation, Inc

In collaboration with
Ronald Smolowitz – Coonamessett Farm Inc.
Tor Bendiksen – Reidar's Manufacturing, Inc.
Fredrick Thwaites – Woods Hole Oceanographic Institution
Centre for Sustainable Aquatic Resources, Memorial University

Coonamessett Farm Foundation, Inc

277 Hatchville Road
East Falmouth, MA 02536

508-356-3601 FAX 508-356-3603
contact@cfarm.org

www.cfarm.org

Project Title: Improving a Low Profile Dredge Using Computational Fluid Dynamics and Flume Tank Testing

Principal Investigators: Liese Siemann and Farrell Davis

Organization: Coonamessett Farm Foundation, Inc.

NOAA Grant Number: NA17NMF4540036

Report date: May 29, 2018

Executive Summary

Coonamessett Farm Foundation designed and tested a variety of low profile dredge (LPD) prototypes between 2012 and 2015. Based on the results of fishing trials, we suspected that the first LPD prototype dredge was flying rather than making contact with the sea floor because catch rates for scallops and fish were low. The dredge was redesigned with the aid of computational fluid dynamics (CFD) models and tested at sea in 2015. Analysis of the fishing trials with the redesigned LPD (LPD v2) indicated that it caught scallops at a rate comparable to a commercial turtle-deflector dredge (TDD) while reducing the catch of windowpane flounder. The main objective of this project was to further improve and develop the LPD v2 using CFD analysis and validate the model with flume tank tests using scaled dredge models. Dredge frame modifications can be tested for a fraction of the price of at-sea trials using the methods developed during this project.

Reidar's Manufacturing built a set of dredge frames and dredge bag scaled to 1/6th of the standard dredge size that could be used in flume tanks at scaled speeds that match speeds used in the commercial scallop fishery. The dredge models were tested in the flume tank at the Marine Institute Centre for Sustainable Aquatic Resources (CSAR) at Memorial University in Newfoundland. Tests were conducted with and without a scaled dredge bag attached, and the wire was scaled to be equivalent to a 1 1/8" diameter wire commonly used with scallop dredges. A range of speed and wire scope combinations were tested, and the bale angle was measured for the full range of speeds and wire scopes for each dredge using a calibrated camera on a trolley. The wire was marked at 1-meter intervals so the shape of the catenary could be plotted, and a load cell was attached between the side of the tank and the wire to measure changes in wire tension with dredge type, wire scope, and speed. Fluorescent dye tablets, yarn telltales, and scaled scallops were used to visualize the flow and any turbulence behind the dredge frames.

Flume tank results were compared to the results from CFD models run by CFF. Simulation output was examined using animated cut plots of turbulent energy and pressure, XY-plots of changes in turbulent energy and pressure with distance from the dredge cutting bars, and particle studies that tracked particle movements behind the dredge frames. The results of the CFD simulations successfully highlighted details about dredge hydrodynamics that were observed during flume tank tests.

Based on results from the flume tank tests and CFD simulations, we suspected that turbulence behind the LPD v2 might contribute to its lower efficiency relative to the standard-height frames. Therefore, we created two more LPD variants to reduce turbulent flow relative to the LPD v2 by shortening the depressor plate and reducing the depressor angle. Both new LPD variants are very promising, and both could improve dredge selectivity, increasing the capture of large scallops and the escapement of small scallops.

It may be difficult to overcome consequences of highly turbulent flow behind shorter dredge frames because interactions between flow fields generated by dredge depressor plates and the sea floor cannot be avoided. Consequently, further improving LPD efficiency may require a new dredge bag design. Observations during this project indicated that the dredge bag was not opening as expected. If this observation holds true for full-sized dredge bags used by the scallop fleet, the consequences include reduced fishing efficiency, decreased mechanical sorting and size selectivity of scallop catch, and reduced escapement of bycatch species. Designing and testing new dredge bags is a logical next step in our efforts to improve scallop dredges using flume tank tests and CFD modeling.

Project timeline

Funding period: March 1, 2017 - February 28, 2018

Kick-off meeting: April 5, 2017 (attended by L. Siemann, F. Davis, R. Smolowitz, T. Bendiksen, and F. Thwaites)

CFD simulations: CFD simulations were conducted periodically from March 2017 through January 2018

Scaled dredge development: Discussions about dredge design occurred from April – August 2017. Dredges were finished by September 10, 2017.

Flume tank testing: September 15 – 23, 2017 (trip participants included L. Siemann, F. Davis, R. Smolowitz, T. Bendiksen, C. Quinn, and E. Welch)

Meeting to review CFD and flume tank results: December 15, 2017 (attended by L. Siemann, F. Davis, R. Smolowitz, and F. Thwaites)

Project management and participation

Project management and data analysis: Liese Siemann.

CFD simulations: Liese Siemann, with assistance from Farrell Davis and Fred Thwaites.

Modular scaled dredge design and construction: Tor Bendiksen, with assistance from Farrell Davis, Liese Siemann, and Ron Smolowitz

Flume tank testing: Liese Siemann, Farrell Davis, Ron Smolowitz, Tor Bendiksen. Charlie Quinn (Quinn Fisheries), and Eddie Welch (F/V Westport). Dredge evaluations were carried out by George Legge and Tara Perry (Marine Institute, Memorial University).

Background

The Atlantic sea scallop (*Placopecten magellanicus*) is the focus of one of the most valuable fisheries on the east coast of the United States (NEFSC 2014). Yet the incidental bycatch of pre-recruit scallops and non-target species could have negative impacts on the long term sustainability of the scallop fishery. Years of high recruitment of sea scallops within the rotational access areas has created a situation where high abundances of pre-recruit and harvestable scallop resources are found together. Furthermore, bycatch of certain species, such as yellowtail flounder (*Limanda ferruginea*) and windowpane flounder (*Scopthalmus aquosus*), are impacting catch levels and quota, thereby putting the continued sustainability of the fishery at risk (O'Keefe & DeCelles 2013). Coonamessett Farm Foundation (CFF) has been at the forefront of developing important scallop dredge modifications that have been incorporated in the scallop management frameworks to reduce fish and sea turtle bycatch while maximizing scallop catch. Yet, the development and testing of each gear modification costs hundreds of thousands of dollars due to expensive at-sea testing. During the last five years, CFF gear projects have cost an average of $270,000 each.

Computational fluid dynamics (CFD) analysis offers a low-cost alternative to at-sea testing of preliminary gear modifications. When used together, flume tank and CFD analysis can effectively predict the flow velocities and pressures that influence fishing gear performance (Meyler 2008). CFD analysis has been used optimize trawl door designs (Hermannsson 2014), and when CFD and flume tank studies have been conducted on the trawl designs, results from the two analyses have been comparable (Nguyen et al. 2015). Furthermore, results from both analyses have predicted the main performance parameters of the trawls during at-sea fishing trials (Nguyen et al. 2015).

Previous research

CFF designed and tested a low profile dredge (LPD) prototype in 2012 with funding from the scallop RSA program (NA11NMF4540021) (**Figure 1A**). Based on results of the fishing trials, we suspected the dredge was flying rather than making contact with the sea floor because catch rates for scallops and fish were very low. The original LPD prototype (LPD v1), with the depressor plate attached along the top side of the struts, had a depressor plate angle of 22 degrees (**Figure 1A**). We hypothesized that LPD v1 performance could be improved by dropping the depressor plate between the struts to increase the angle of the depressor plate to 45 degrees, matching the angle in standard-height dredges (LPD v2) (**Figure 1B-C**).

Figure 1. (A) First low profile dredge prototype (LPD v1) with a 22° depressor plate (B) Standard-height turtle-deflector dredge (C) Redesigned low profile dredge (LPD v2) with a 45° depressor plate. The depressor plates are highlighted in red.

After redesigning the geometry of the depressor plate, CFF contracted with the Marine Institute Centre for Sustainable Aquatic Resources (CSAR) at Memorial University in

Newfoundland to run CFD simulations on the original and modified LPD frames (LPD v1 and LPD v2) prior to building the new dredge and conducting at-sea testing. The simulations were run with 15° bale angles, based on tilt-sensor data we collected in the field. These simulations showed that LPD v1had a low drag coefficient and streamlined flow (**Figure 2A**), while LPD v2 generated a complex flow pattern with a strong vortex behind the cutting bar that resulted in flow up and into the dredge (**Figure 2B**).

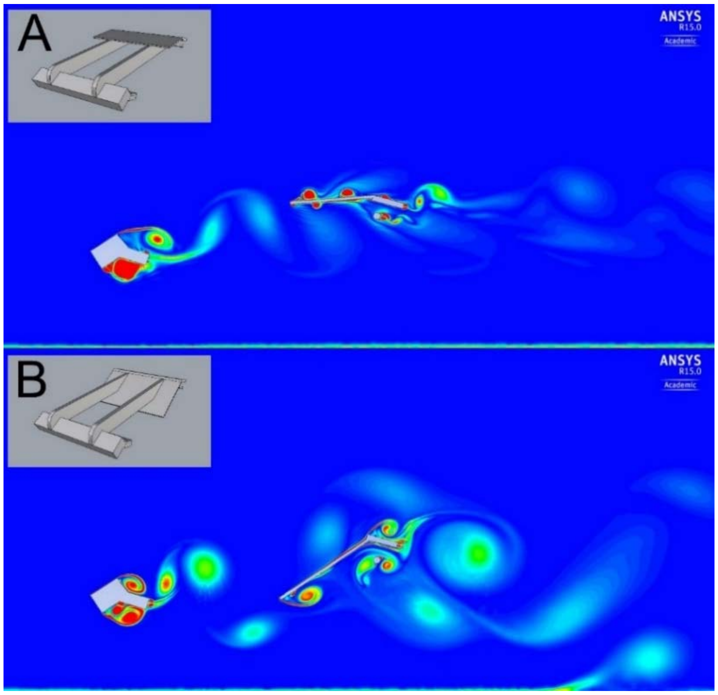

Figure 2. Output from the computational fluid dynamics simulation in ANSYS Fluent showing (A) the vortex contours for the original low profile dredges and (B) the vortex contours for the redesigned low profile dredge.

While the LPD v1 caught significantly fewer flounder relative to standard-height turtle-deflector (TDD) and New Bedford dredges (NBD) (15-19% reductions for windowpane, winter, and yellowtail flounders), scallop catch was also reduced by 10% in the LPD v1 relative to the TDD and NBD. Analysis of the fishing trials with the redesigned LPD v2 indicate that it catches scallops at a rate comparable to a TDD while reducing catch of windowpane flounder (**Figure 3**). However, the LPD v2 still needs improvements. The observed reductions in flounder catch were not significant because there was considerable variability between trips. By using CFD analysis, validated with flume tank tests, we can test additional dredge frame modifications for a fraction of the price of at-sea trials.

Objectives

The project objectives included:

(1) Developing a modular scaled dredge to examine the impacts of changing the geometries of scallop dredges.

(2) Testing the scaled dredge in multiple configurations in a flume tank at scaled speeds that match realistic fishing speeds, and

(3) Simulating the performance of different dredge configurations using CFD models.

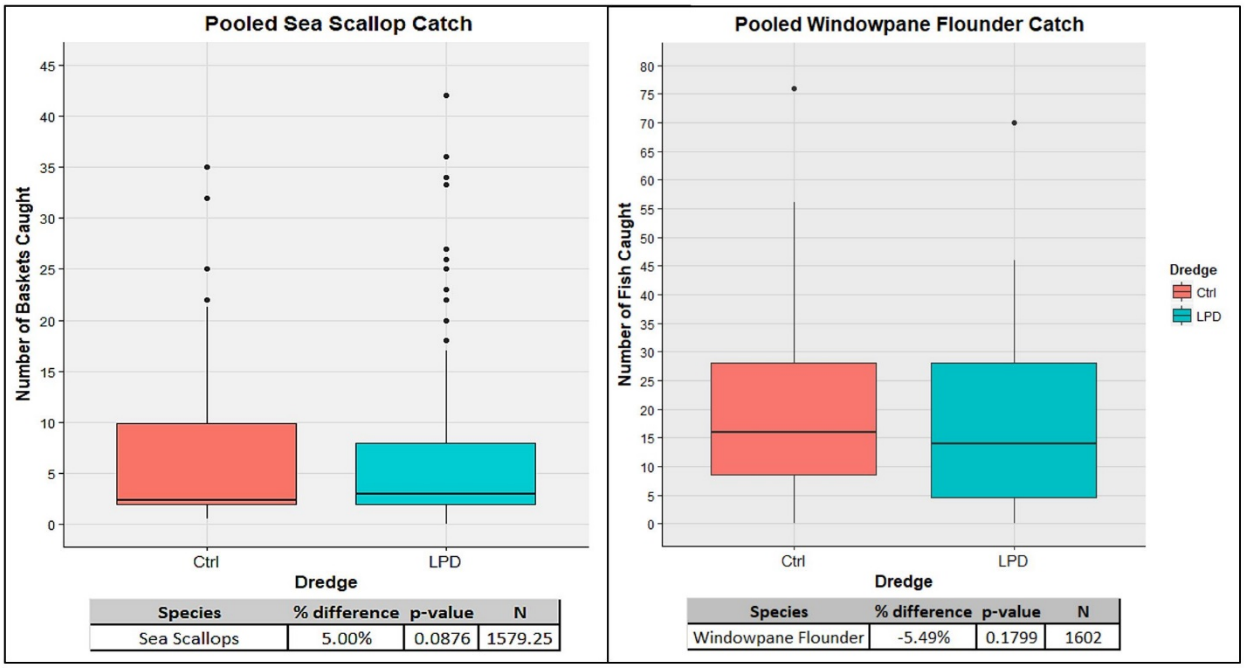

Figure 3. Boxplots comparing differences in the pooled catches of scallops and windowpane flounder from three research trips that tested the LPD v2. The bold line represents the median catch per tow. P-values were obtained using a Mann/Whitney signed-rank test. From Davis et al. 2017.

Methods by Objective

Design and development of scaled dredges

Three scaled dredges were built by Reidar's Manufacturing. The flume tank has a maximum flow speed of ~2 knots. Therefore, in order to test a model dredge at scaled fishing speeds of 4.8-5 knots, our model had to be approximately 1/6th normal size (scaled speed = speed x $\sqrt{\text{scale}}$) (scaled by Froude number - Heller 2011).

Originally, we planned to build a single dredge that could be modified by exchanging the depressor plates and a middle unit that corresponded to a New Bedford dredge (NBD), a turtle deflector dredge (TDD), and the LPD v2. This plan was modified because the dredge geometries were too dissimilar. Instead, three scaled dredges were built: an NBD, a TDD, and an LPD with top units that could be exchanged to represent two versions of this dredge (LPD v1 and LPD v2) (**Figure 4**).

The linear dimensions of all three dredges were scaled to 1/6th the size of a commercial dredge, with the weights also scaled as closed as possible to this ratio. In addition, a 7-row apron dredge bag, scaled to the correct 1:6 size and weight, was built to allow testing of the dredges with and without bags attached (**Figure 5**).

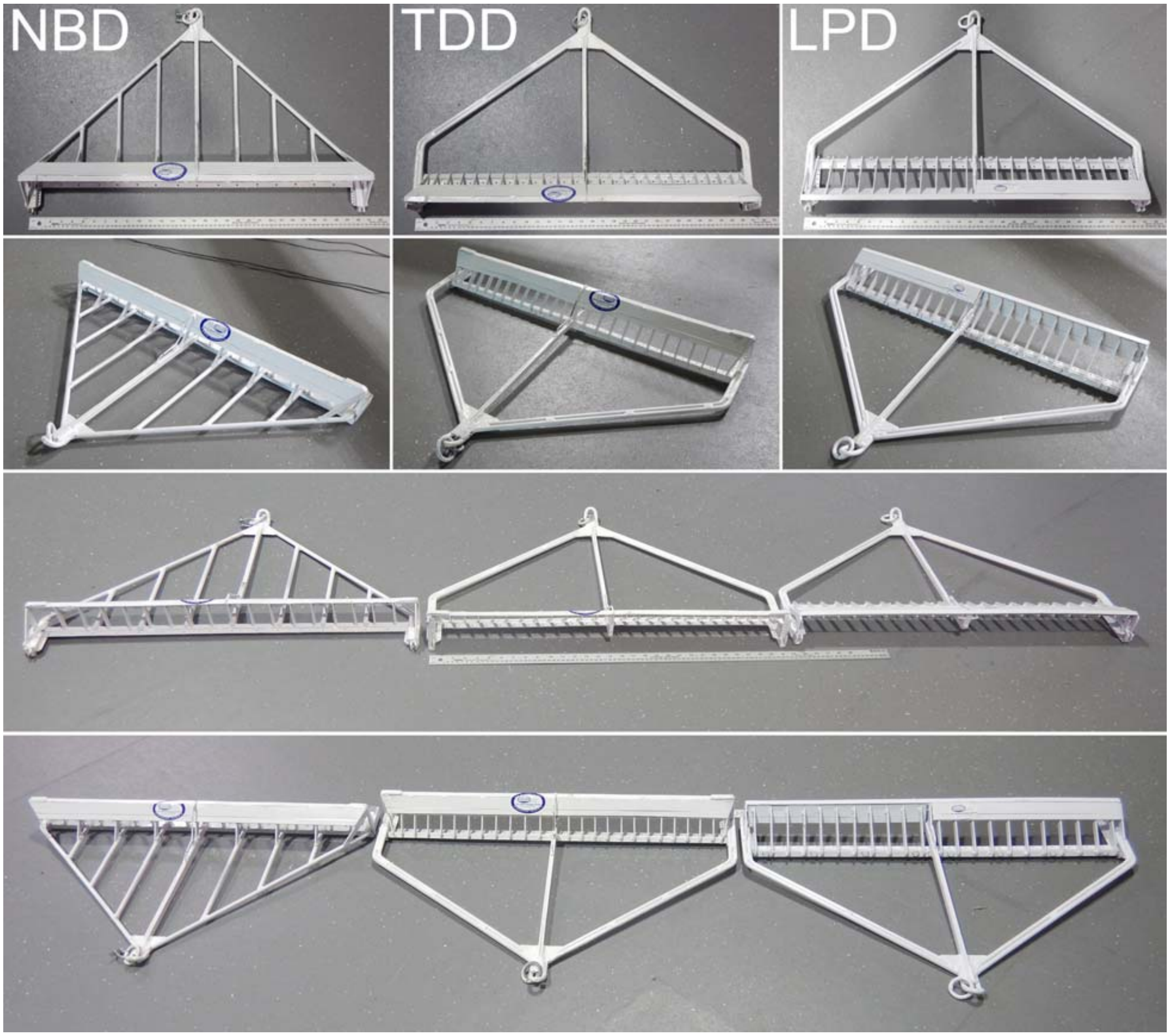

Figure 4. Scaled dredges used for flume tank testing. All dredges were built to 1/6th scale. A meter stick is shown for scale. The LPD is shown with the 22-degree (LPD v1) and 45-degree (LPD v2) depressor plates to highlight the difference between these configurations.

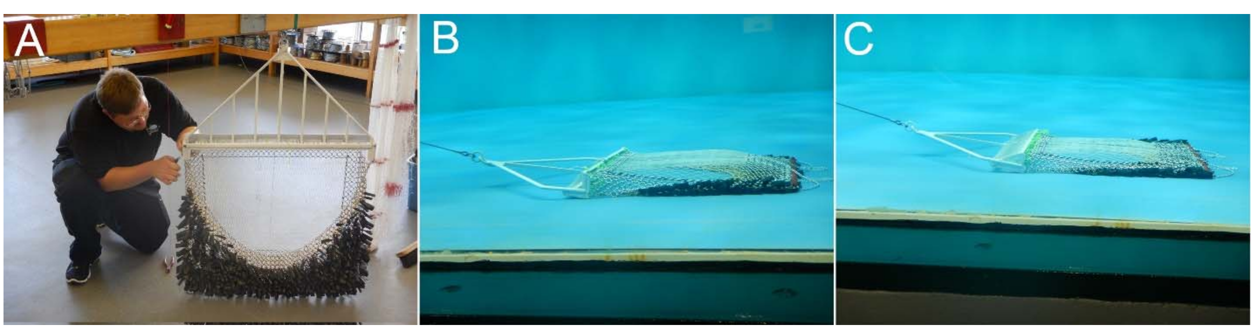

Figure 5. Scaled 7-row apron dredge bag. (A) Tor Bendiksen of Reidar's Manufacturing hangs the bag on the NBD. (B) Bag attached to the TDD during flume tank testing. (C) Bag attached to the LPDv2 during flume tank testing.

Testing of scaled dredges in a flume tank

The scaled dredges were tested in the flume tank at CSAR (**Figure 6**). Tests were conducted with and without a scaled dredge bag attached. The wire was scaled to be equivalent to a 1 1/8" diameter wire commonly used with scallop dredges. Yarn telltales and scaled scallops were used to indicate flow direction (**Figure 7**). The scaled scallops were made by gluing scallop seed shells together, with seed shells donated by Nate Perry, owner of Pine Point Oysters in Maine. The shells were attached to threads that were 1.5", 3", 6", and 16" long, with the longest threads ending just before the start of the sweep in the scaled bag, and tied to the cutting bar.

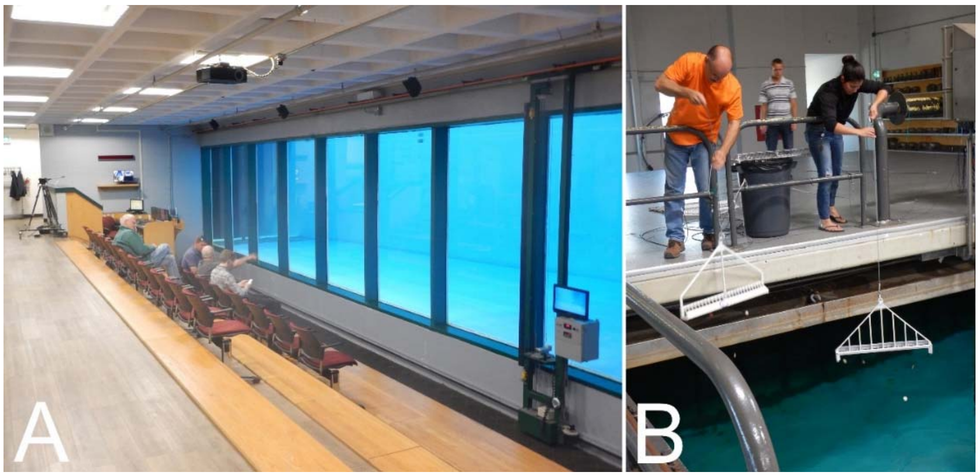

Figure 6. The flume tank and the Marine Institute. (A) The tank viewing area. (B) Lowering the TDD and NBD into the tank.

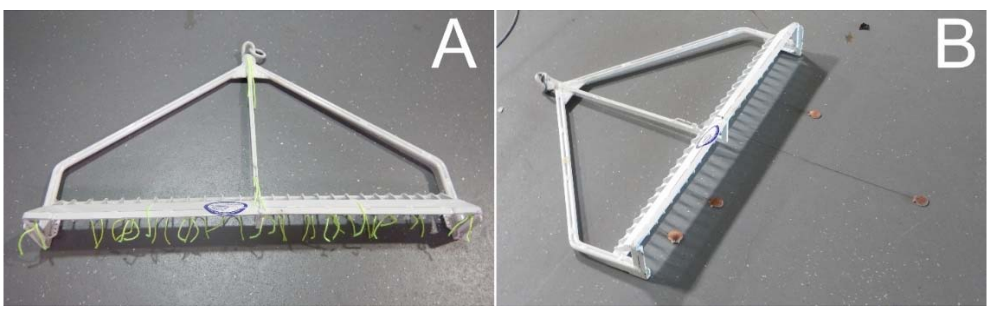

Figure 7. TDD with (A) yarn telltales and (B) scaled scallops attached.

A range of speed and wire scope combinations were tested for all of the dredges and both LPD configurations with and without bags (**Table 1**). The first tests were conducted with the NBD and a short 2.5:1 scope and scaled speeds ranging from 2.5 to 5.5 knots at 0.5 knot intervals. The maximum speed available in the tank was a scaled speed of 5.5 knots. Based on the results of this first series of tests, other dredges were tested with a 3:1 scope at 3, 4, 5, and 5.5 knots. Scopes beyond 3:1 were not tested to keep the dredges from reaching the back of the test tank. The bale angle was measured for the full range of speeds and wire scopes for each dredge using a calibrated camera on a trolley (**Figure 8A**). In addition, the wire was marked at 1-meter intervals, and the X-Y coordinates of each mark were measured for a series of tests so the shape of the catenary could be plotted, and trends in the change of this shape could be examined for each dredge type and scaled speed (**Figure 8B**). A load cell was attached between the side of the tank and the wire to measure changes in wire tension with dredge type, wire scope, and speed. To visualize the flow and any turbulence behind the dredge frames, fluorescent dye tablets were glued to the frames on the bale angle bars and on the cutting bar. These images were visually compared to the results from the CFD models.

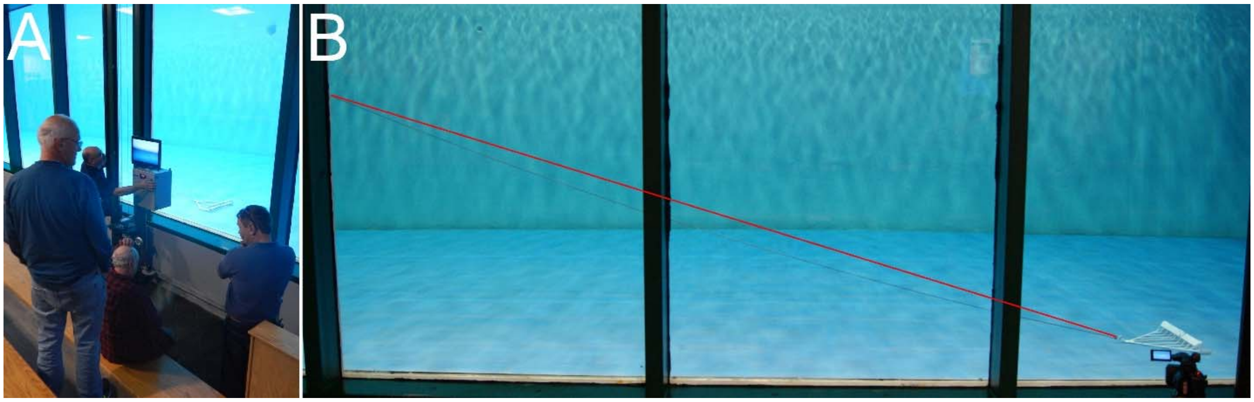

Figure 8. (A) Trolley-mounted camera used to measure the bale angle and catenary shape. (B) Example of wire catenary. The red line is straight, while the wire hangs below to forms a curve determined by the dredge speed and drag and the wire length.

Modeling dredge performance using CFD simulations

Flow around the different dredges was modeled using the Flow Simulation package for SOLIDWORKS using CAD drawings for full-sized dredges. This package uses Cartesian-based meshes with rectangular cells that can arbitrarily intersect with the solid bodies, and the CFD equations are solved using modified k-ε models focused on turbulent kinetic energy (Sobachkin & Dumnov 2014). Because simulations are computationally demanding, all modeling was done on a machine with an Intel Xeon processor, 64GB of RAM, and a dedicated NVIDIA graphics card. Flow Simulation settings for 2D runs are shown in **Table 2** and **Figure 9**.

Initially we ran simulations with bale angles ranging from 10 to 20 degrees, based on tilt-sensor data we collected in the field. This allowed us to compare out results to those generated by CSAR using different software (ANSYS Fluent). However, we suspect that our tilt sensors may not be measuring these angles correctly. Consequently, to determine if the results of the CFD models approximate real flow around a dredge, we ran simulations with the speeds and corresponding bale angles we observed in the flume tank during dye tests. For all dredge frames, we also ran simulations with a 5° bale angle, which was close to the observed values in the flume tank with bags attached. In addition to running simulations with dredges that matched the specifications of the scaled model dredges, we ran simulations with two more modified LPDs at 5° bale angles: (1) an LPD with a 6-inch depressor plate (vs the normal 10-inch plate) at a 45° angle (LPD short) and (2) an LPD with the normal 10-inch depressor plate shifted to a 30° angle (LPD 30).

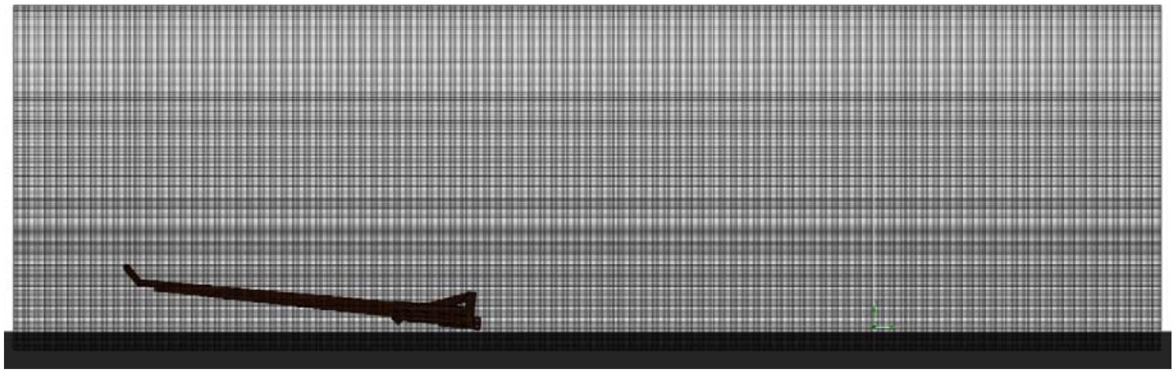

Figure 9. Computational domain and mesh used for simulations. The fine mesh effectively captured flow details around the dredge frames.

Simulation output was examined in three ways.

(1) Cut plots that summarized turbulent energy, vorticity, and relative pressure were generated from the CFD models for each dredge type (see **Table 3** for details). These plots give colorimetric summaries of flow properties. Because we ran time-dependent simulations, the cut plots could be animated to show changes in flow properties over time (animations are available upon request).

(2) Changes in turbulent energy and pressure were plotted against distance from a point immediately in front of the cutting bar of each dredge. To generate these XY-plots, a line that cuts across the models had to be selected. For comparisons between the NBD, TDD, LPD v1, and LPD v2, a line located 8 cm off the bottom was used because it intersected with the cutting bars of all four dredges. For further comparisons between the TDD, LPD v2, LPD short, and LPD 30, a line 5 cm off the bottom was selected for all four dredges. This line intersected with the middle of the LPD cutting bars. But because the TDD has taller shoes, the 5-cm line skimmed the bottom edge of the cutting bar, so a second line 10 cm off the bottom was used to intersect with middle of that cutting bar.

(3) Particle studies were done to investigate the behavior of the scaled scallops behind the NBD and TDD dredge frames. Because these scallops approximated the size of large scallops relative to the dredge models, these studies used large particles with start locations that covered the range of scaled attachment distances used in the flume tank tests (**Table 4**). Bale angles matched those observed in the test tank and used for the cut plot analyses. A second set of particle studies, with injections in front of the cutting bar, were used to investigate how particles of different sizes, representing large and small scallops, would travel in the flow field behind the NBD, TDD, LPD v2, LPD short, and LPD 30 (**Table 4**). For this analysis, all dredges had the same bale angles, all close to those observed in the flume tank with bags attached.

Results

Testing of scaled dredges in a flume tank

Flow around the frames was visualized during testing using yarn telltales and scaled scallops. The telltales were sucked forward through the struts of the NBD (**Figure 10A**), while they continued to flow behind the TDD and LPD frames (**Figure 10B-D**), suggesting the flow patterns behind the

NBD are different than those behind the other dredges. This difference in flow patterns was further confirmed using the scaled scallops. While the scallops attached to the TDD bounced around and rose into the water column behind the frame, the scallops behind the NBD were repeatedly sucked into the cutting bar (**Figure 11**).

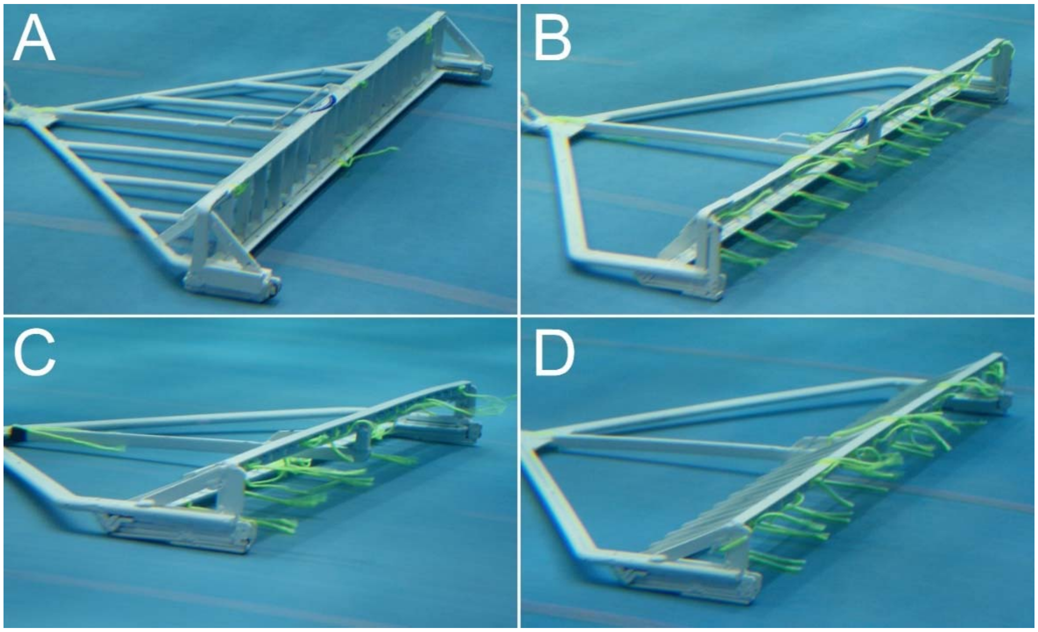

Figure 10. Telltales behind (A) the NBD, (B) the TDD, (C) the LPD v1, and (D) the LPD v2. Note that there were fewer telltales attached to the NBD because additional yarn was added after the initial tests.

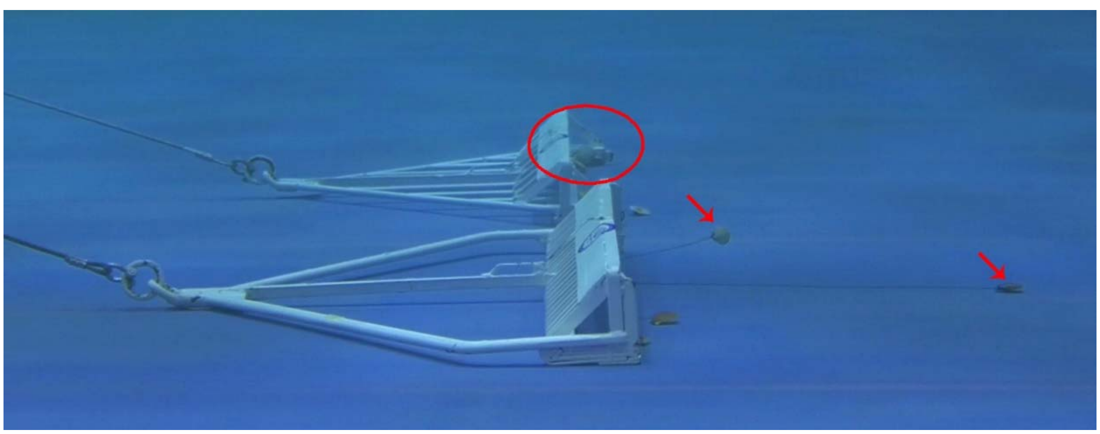

Figure 11. Scaled scallops behind the TDD (front) and the NBD (back). Scallops bounced behind the TDD (red arrows), while they were sucked into the cutting bar behind the NBD (red oval). Both dredges had 2.5:1 wire scopes, so the different locations were due to different catenary shapes, with the NBD wire hanging lower in the water than the TDD wire.

Observations of the scaled bag were also illuminating. While the bag opened up and behaved as expected when towed behind the TDD, it remained flat when towed behind both LPD frames (**Figure 12**). Expansion of the bag behind the NBD was similar to that behind the TDD. However, even when the bag expanded behind the TDD, the corners remained flat, suggesting the bag may not be as efficient as possible.

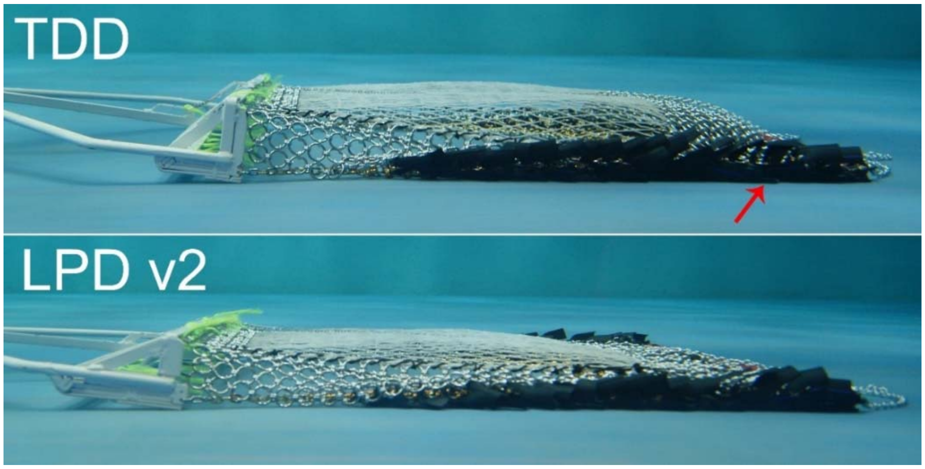

Figure 12. The scaled dredge bag pulled behind the TDD and the LPD v2 (3:1 scope at 5.5 knots). Note that the bag did not open fully in the corners (red arrow).

Measurements taken during flume tanks tests are summarized in **Tables 5 and 6**. As expected, warp tensions were higher on dredges with bags than dredge frames alone (**Figure 13**). While the LPD v1 dredge frame had noticeably lower warp tensions than other dredge frames at all speeds, this difference was no longer apparent when the dredge bag was attached. Warp tensions for the LPD v2 were similar to those of the TDD and NBD. Catenary shapes for all dredges were similar, with the LPD v1 having a more curved shaped consistent with lower warp tensions (**Figure 14**). In general, bale angles increased with increasing speeds (**Figure 15**). The bale angles for the dredge frames alone stayed constant from 3 to 4 knots for the NBD and LPD frames and from 3 to 5 knots for the TDD frame, indicating that downward forces from the depressor plates counteracted lift at lower speeds. The addition of the dredge bag altered this effect. The bale angle decreased from 3 to 4 knots for the NBD and TDD and then increased from 4 to 5.5 knots when the bag was attached. While the bale angle increased overall for the two LPD frames with bags attached, it dipped at 5 knots for both frames.

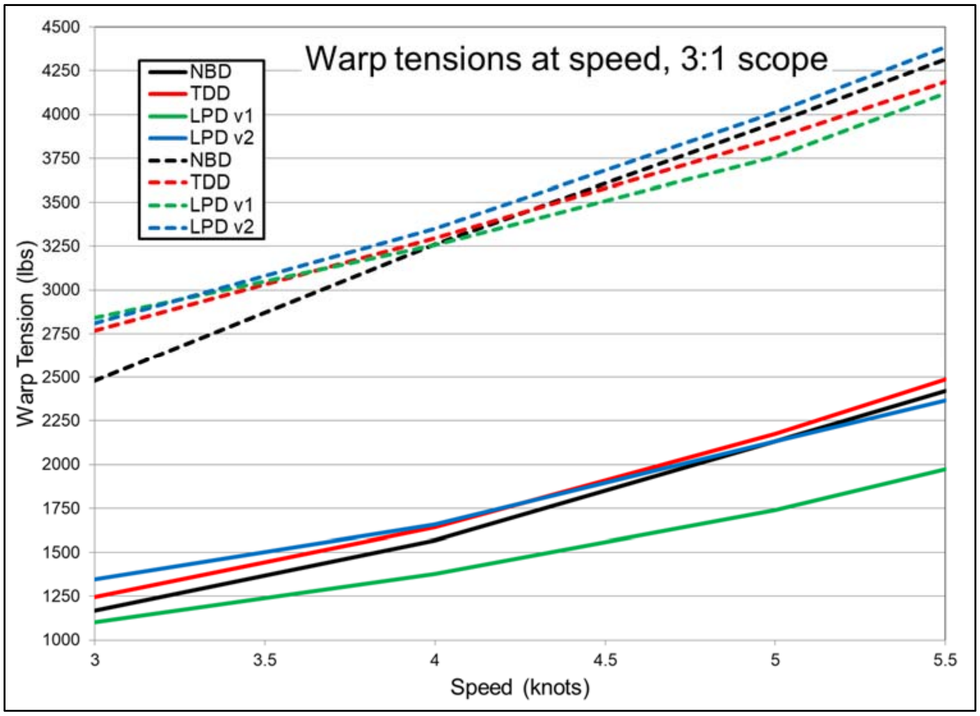

Figure 13. Warp tensions at speeds from 3 to 5.5 knots (scaled speeds) with 3:1 scopes.

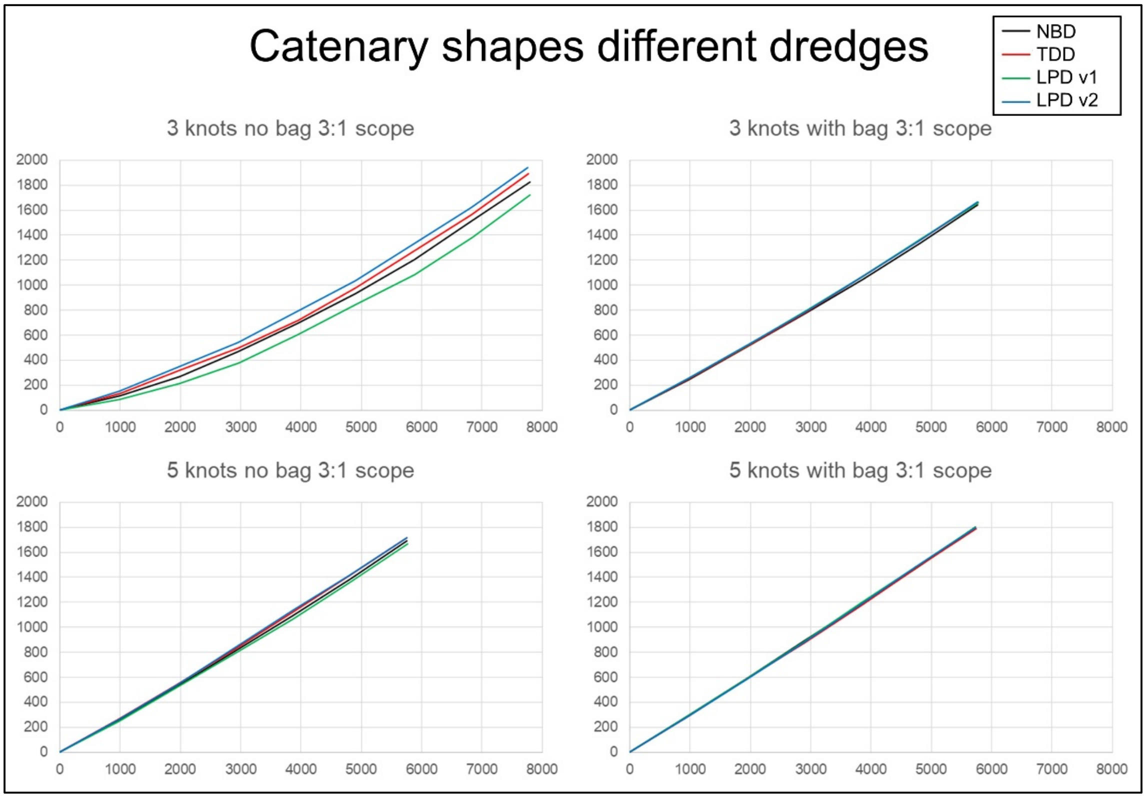

Figure 14. Catenary shapes for the different dredges with 3:1 scopes at 3 and 5 knots. Units on the axes are the X and adjusted Y coordinates shown in Table 5.

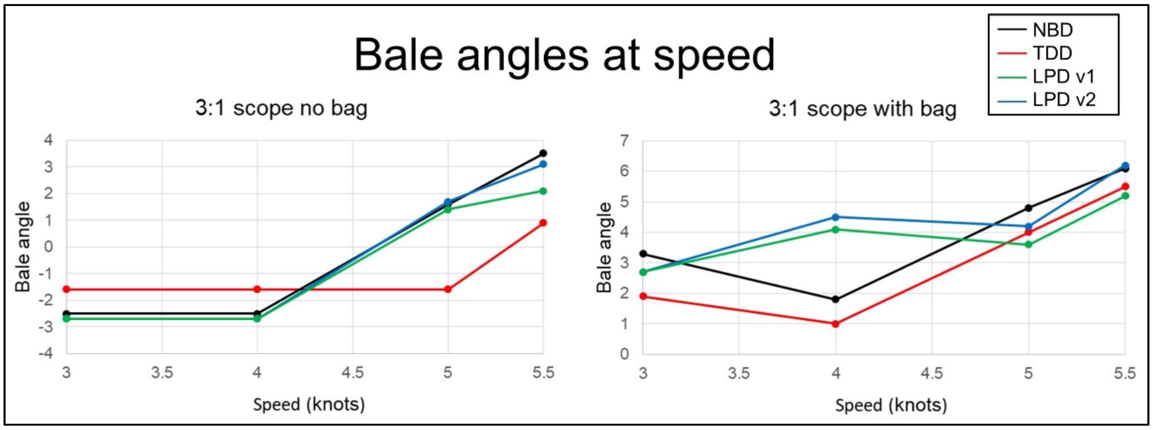

Figure 15. Changes in bale angles with speed for dredges with 3:1 scopes.

Modeling dredge performance using CFD simulations

The simulations used to validate the use of CFD modeling for dredge design were run at 5 knots with the bale angles measured during flume tank dye tests (**Table 5**). Because turbulent flow is clearly visualized by examining turbulent energy, CFD cut plots of these values were compared to images of the dye streams behind each scaled dredge during flume tank testing (**Figure 16**). The trends in the magnitude of the turbulence predicted by the CFD models for each dredge type were consistent with what was observed in the flume tank. The magnitude and intensity of the turbulent flow was highest for the LPD v2, moderate LPD v1, and lowest for the NBD and TDD. Interaction with the bottom contributed significantly to the turbulence behind the two LPD frames.

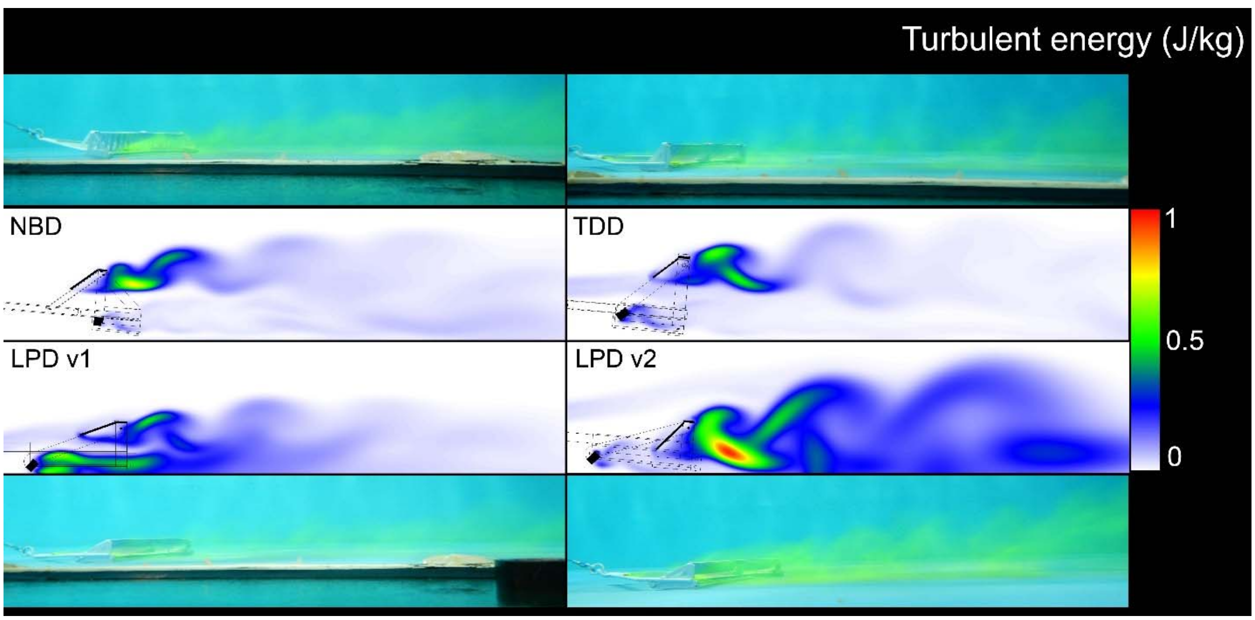

Figure 16. Representative turbulent energy cut plots from CFD models for each dredge type. Images of the dye streams behind each dredge during flume tank testing are also shown immediately above or below each cut plot.

Plots of the turbulent energy 8 cm off the bottom (from in front of the cutting bar to 4 meters behind the cutting bar) confirm the observations from the cut plots and dye tests (**Figure 17**). Turbulent energy behind both LPD frames were higher than behind the NBD and TDD, with turbulent flow continuing to persist 4 meters behind the LPD v2. This contrasted with turbulence that decreased to minimal levels behind the taller NBD and TDD.

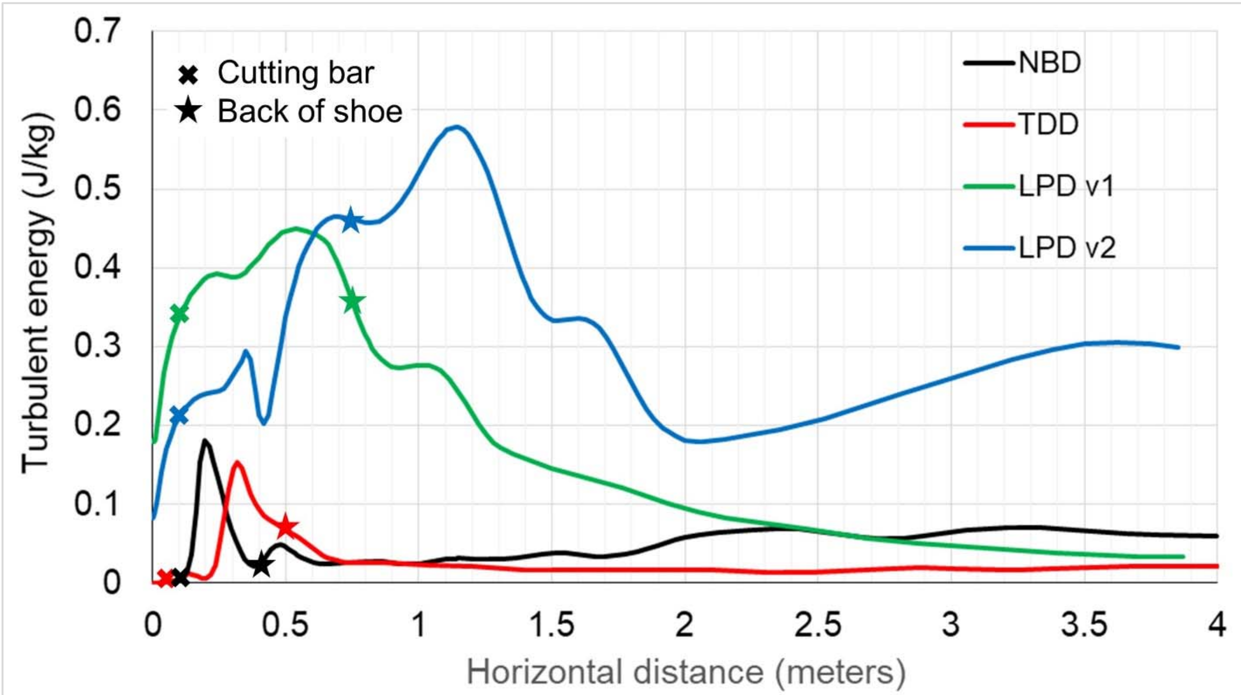

Figure 17. Turbulent energy around and behind each dredge along a line placed 8 cm off the bottom.

There were areas of high pressure in front of and low pressure under and behind each depressor plate (**Figure 18**). Interestingly, there was a larger low pressure region behind the cutting bar of the NBD relative to the TDD, which may have contributed to the observation of scaled scallop shells being repeatedly sucked into the cutting bar of the NBD during the flume tank tests. Plots of the pressure 8 cm off the bottom indicate that the regions of lowest pressure for the NBD, TDD, and LPD v2 lie between the cutting bar and the back of the shoe (**Figure 19**). However, the low pressure region generated by the LPD v2 extended 4 meters behind the cutting bar, while the pressures behind the other dredges approached the background reference pressure within 1.5 meters behind the cutting bar.

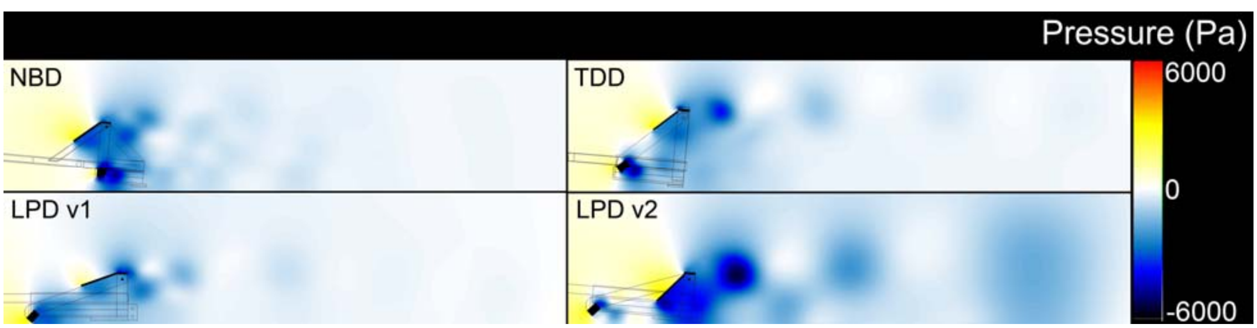

Figure 18. Representative relative pressure cut plots from CFD models for each dredge type

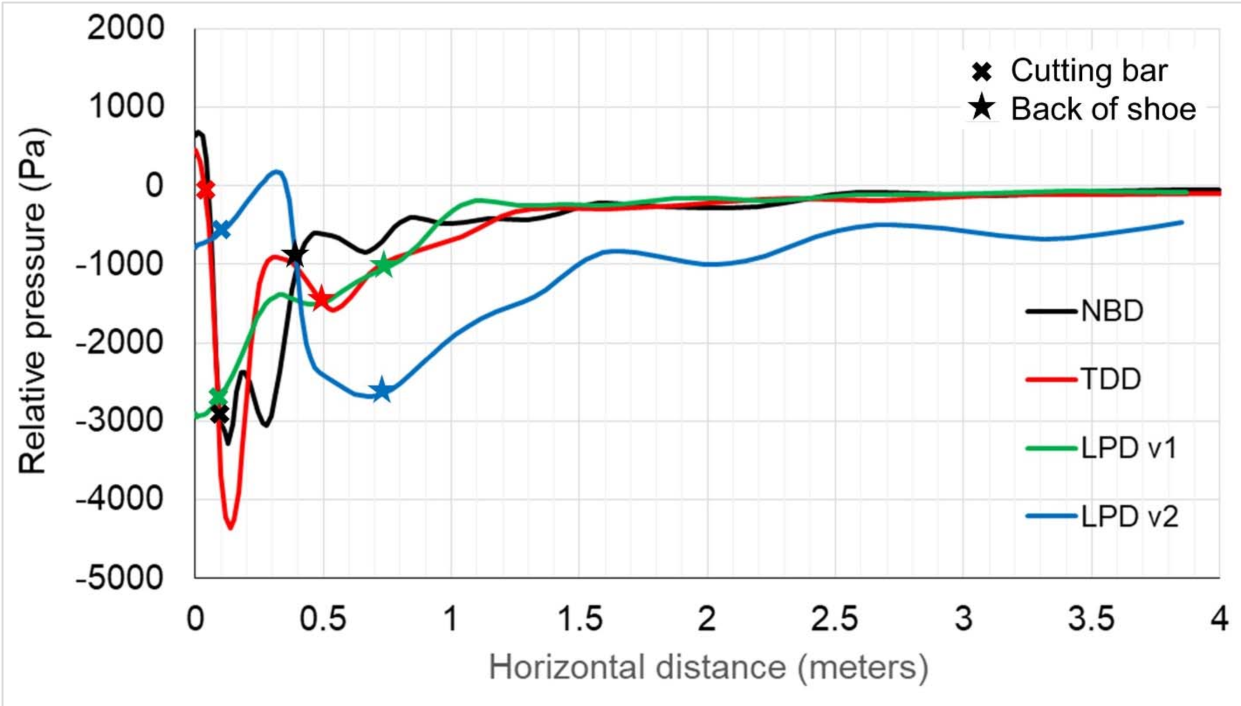

Figure 19. Relative pressure around and behind each dredge along a line placed 8 cm off the bottom.

Particle studies showed that the behavior of the scaled scallop behind the NBD and TDD could be explained based on the modeled flows. While particles injected closely behind the cutting bar of the NBD were caught in an eddy, all particles injected behind the TDD moved upward (**Figure 20**).

Particle studies also provided the simplest visualization of the functional differences between the standard-height dredges and the LPD v2 (**Figure 21**). Large and small particles moved upward behind the NBD and TDD, indicating that flow behind these dredge frames may lift scallops up into the dredge bag. However, particle movement behind the LPD v2 was more complex due to the highly turbulent flow behind that dredge frame. Large and small particles were caught in an eddy located above and behind the dredge frame.

Based on these results, we suspected that turbulence behind the LPD v2 might contribute to its lower efficiency relative to the standard-height frames. Because the flow behind the LPD v2 is dominated by movement up and into an eddy above the dredge frame, scallops may be lifted out of the dredge bag through the twine top and flow into the bag may be reduced. Therefore, we created two more LPD variants, hoping to reduce turbulent flow relative to the LPD v2. By either shortening the depressor plate or reducing the depressor angle, we tried to create a low-profile frame that lifted particles behind the dredge into the bag like the NBD and TDD. Plots of the turbulent energy 5 cm and 10 cm off the bottom confirmed that the turbulent energy of the flow around the new variants was reduced relative to the LPD v2, but higher than the TDD (**Figure 22**). However, while predicted particle movements behind both new LPD variants were not similar to those behind the standard-height frames, both frames may improve dredge selectivity. The simulations indicated that large scallops would be held in eddies just behind and under the depressor plate for capture, while small scallops would be lifted out through the twine top (**Figure 21**).

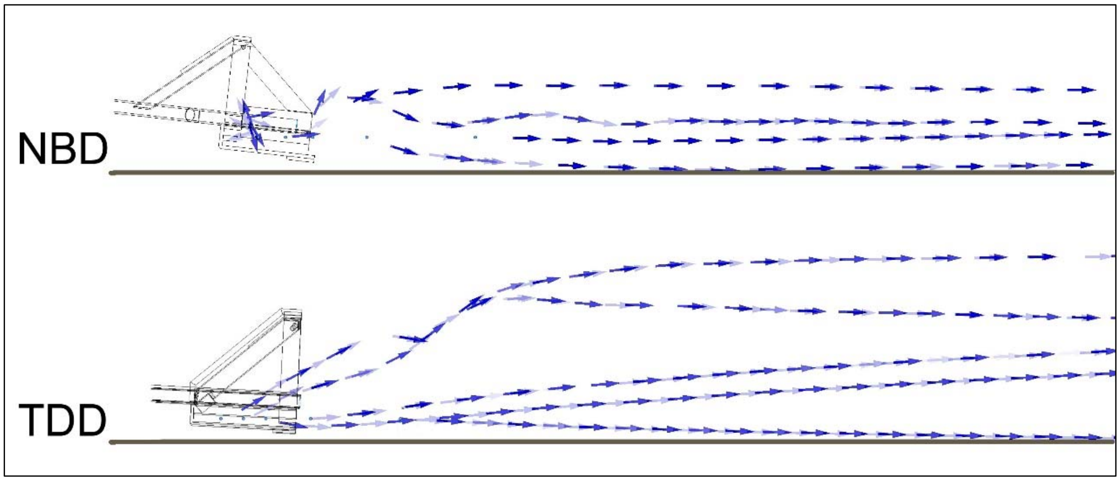

Figure 20. Particle movement behind the NBD and TDD frames predicted using particle studies based on CFD simulations. Particle tracks show the movements of large particles (100-cm diameter) injected at locations that covered the range of scaled attachment distances used in the flume tank tests with scaled scallops.

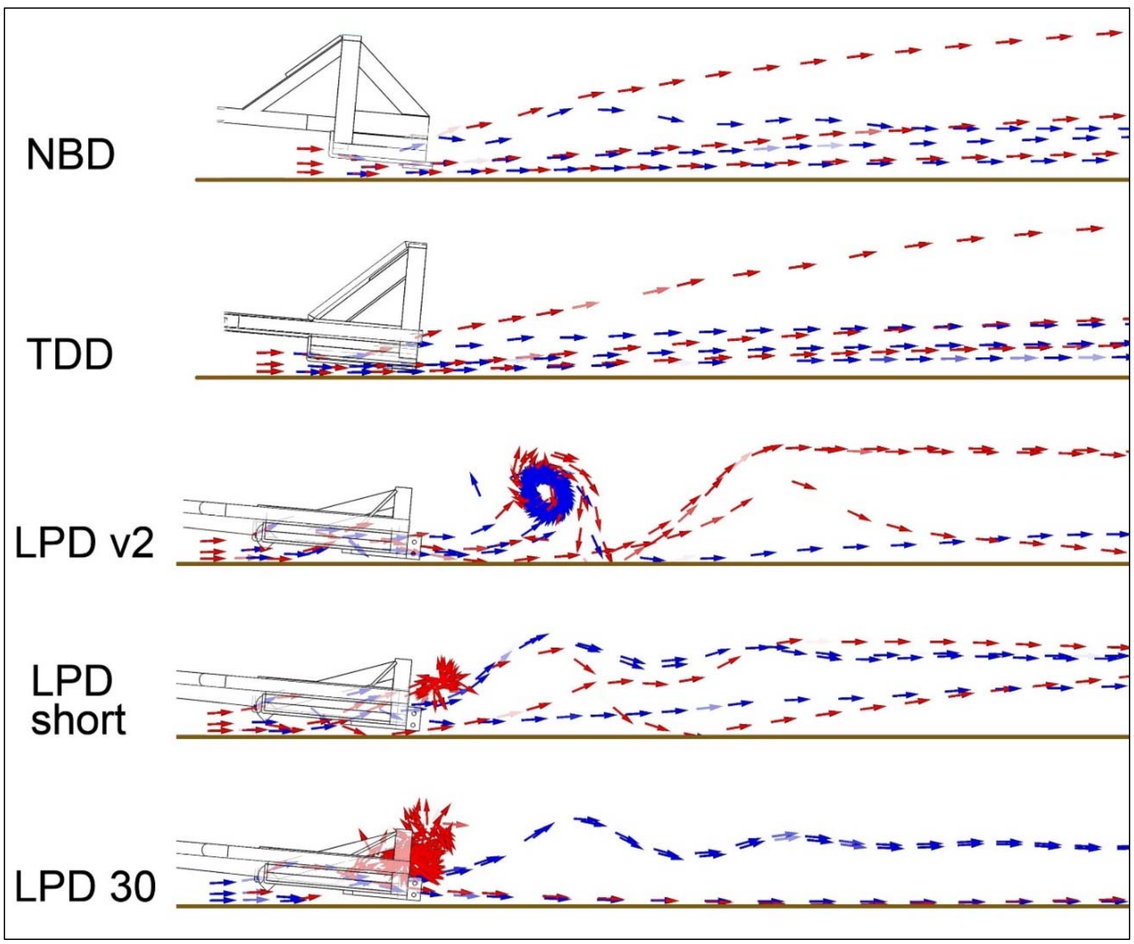

Figure 21. Particle movement behind dredge frames predicted using particle studies based on CFD simulations. Particle tracks in red show the movements of large particles (100-cm diameter), while particle tracks in blue show movements of small particles (25-cm diameter).

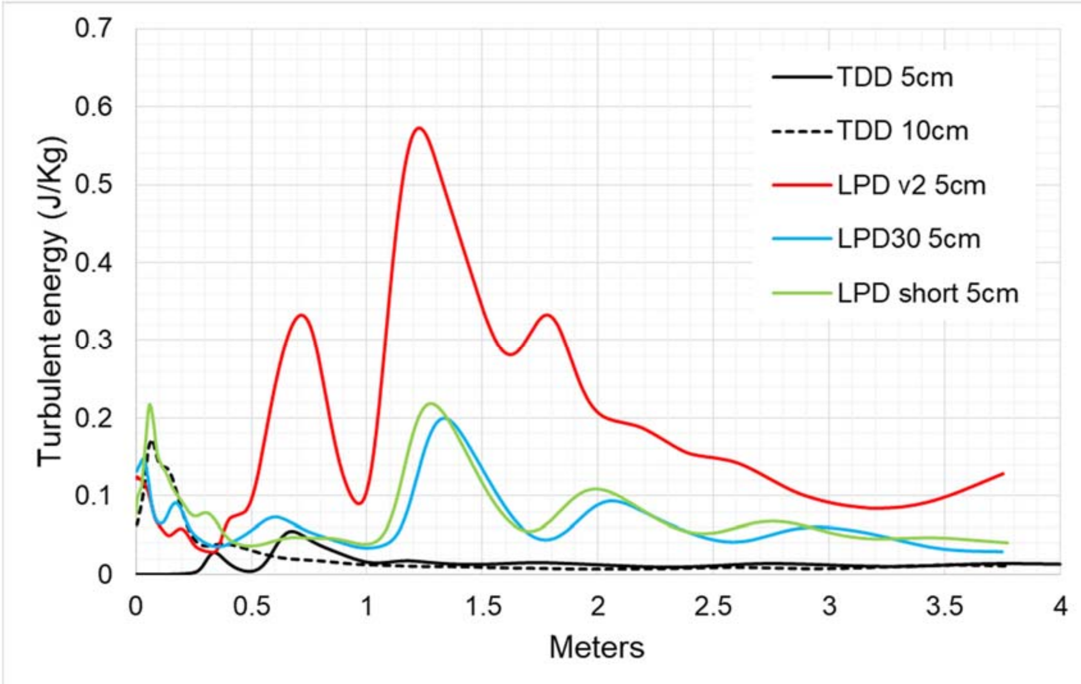

Figure 22. Turbulent energy around and behind the TDD and LPD variants along lines placed 5cm and 10 cm off the bottom.

Evaluation

Accomplishments by objective

All objectives were accomplished with few modifications. Accomplishments by objective are described below.

(1) Developing a modular scaled dredge to examine the impacts of changing the geometries of scallop dredges.

We successfully designed and built a set of 1/6th scale dredge frames and a dredge bag that can be used in flume tanks at scaled speeds that match speeds used in the commercial scallop fishery. We plan to continue using these dredges in future projects.

(2) Testing the scaled dredge in multiple configurations in a flume tank at scaled speeds that match realistic fishing speeds.

The flume tank tests went very smoothly. We were able to test all of our dredge frames at a range of speeds, with and without a dredge bag attached. Measurements of warp tensions, catenary shapes, and bale angles provided important data for understanding the functional differences between the dredge frames. The use of dye tablets, yarn telltales, and small scaled scallops allowed us to effectively visualize differences in flow patterns as we altered the speed of the tests for each dredge.

(3) Simulating the performance of different dredge configurations using computational fluid dynamics (CFD) models.

We modeled flow around six different dredge frames, and simulation output was examined using animated cut plots, XY-plots of important flow parameters, and particle studies. The results of the CFD simulations successfully highlighted details about dredge hydrodynamics that were observed during flume tank tests. Furthermore, we were able to easily test two ideas for improving the LPD, and both new variants are promising. LPD selectivity might be improved with both frames.

Discussion

Overall, the project was highly successful. Observations of dredge behavior in the flume tank were illuminating to all present. Until there is a way to watch full-sized dredges operating at commercial speeds, flume tank tests like those we conducted are the best way to see firsthand how the flow fields generated by dredges impact their performance.

The flume tank tests also provided information needed to assess the validity of using CFD simulations to examine dredge hydrodynamics. CFD simulations are not yet routinely used when developing fishing gear modifications, even though flow simulations are routinely used in other industries. Based on the results of this project, we believe that CFD simulations can continue to provide valuable information during the early stages of gear development. Simulations conducted during this project point toward beneficial new modifications to the LPD frame that could improve dredge selectivity, increasing the capture of large scallops and the escapement of small scallops.

Fishing gear innovation is an incremental process, and acceptance of new designs can take time. Yet successful new gear designs have been adopted by the scallop industry, and the widely used TDD was developed using flume tank tests. Although the TDD is required west of 71°W to minimize sea turtle bycatch, it is used in other areas because it is believed to be more efficient on featureless bottom. Innovative new gear designs have been adopted by industry if they improve gear efficiency or reduce bycatch.

Additional Work

While the two new LPD variants we tested using CFD simulations are very promising, it may be difficult to overcome consequences of highly turbulent flow behind shorter dredge frames such as particle/scallop movement up and out of the bag and/or reduced flow into the bag. Interactions between flow fields generated by dredge depressor plates and the sea floor may be difficult to eliminate for a short dredge. Consequently, improving LPD efficiency may require a new dredge bag design.

Observations made during this project indicated that the dredge bag was not opening as expected. If this observation holds true for full-sized dredge bags used by the scallop fleet, the consequences include reduced fishing efficiency, decreased mechanical sorting and size selectivity of scallop catch, and reduced escapement of bycatch species. It is widely thought that fish bycatch reduction is improved in bags that are open with space for fish to move and eventually swim out, and videos taken during fishing and haul back of dredges and trawls show fish swimming in place or in circles for seconds to minutes before escaping through mesh openings. Yet the dredge bag used in the US Atlantic sea scallop fishery has not undergone major redesigns since the 1950s (Bourne 1965), and hydrodynamic forces are necessary to open the naturally flat ring bag currently used in the fishery. Designing and testing new dredge bags is a logical next step in our efforts to improve scallop dredges using flume tank tests and CFD modeling.

Literature Cited

Bourne, N. 1965. A comparison of catches by 3- and 4-inch rings on offshore scallop drags. Journal of the Fisheries Research Board of Canada 22: 313-333.

Davis, F, Smolowitz, R, and Rudders, D. 2017. Improving an ecosystem-friendly dredge. Final report 2015 Saltonstall-Kennedy Grant NA15NMF4270265. 60 pp.

Heller, V. 2011. Scale effects in physical hydraulic engineering models. Journal of Hydraulic Research 49: 293-306.

Hermannsson, E. 2014. Hydrodynamic Shape Optimization of Trawl Doors with Three-Dimensional Computational Fluid Dynamics Models and Local Surrogates. Master's Thesis. KTH Royal Institute of Technology, Stockholm, Sweden. 241 pp.

Meyler, L. 2008. Simulation of net structures hydrodynamic fields. In Petrone, G and Cammarata, G, eds. Modeling and Simulation. I-Tech Publishing. 688 pp.

Nguyen, TX, Winger, PD, Orr, D, Legge, G, Delouche, H, and Gardner, A. 2015. Computer simulation and flume tank testing of scale engineering models: How well do these techniques predict full-scale at-sea performance of bottom trawls? Fisheries Research 161: 217-225.

Northeast Fisheries Science Center (NEFSC). 2014. Stock assessment for Atlantic sea scallops in 2014, updated through 2013. In 59th Northeast Regional Stock Assessment Workshop (59th SAW), pp. 483–782. US Department of Commerce, Northeast Fisheries Science Center. Woods Hole, MA. 483 pp.

O'Keefe, CE and DeCelles, GR. 2013. Forming a partnership to avoid bycatch. Fisheries 38: 434-444.

Sobachkin, A and Dumnov, G. 2014. Numerical basis of CAD-embedded CFD. SOLIDWORKS White Paper. https://www.solidworks.com/sw/docs/Flow_Basis_of_CAD_Embedded_CFD_Whitepaper.pdf.

Table 1. Summary of flume tank tests

Dredge	Scope	Scaled speed (knots)	Catenary measurement	Tension at speed	Bale angle
NBD	2.5	2.5	Y	Y	Y
NBD	2.5	3	Y	Y	Y
NBD	2.5	3.5	Y	Y	Y
NBD	2.5	4	Y	Y	Y
NBD	2.5	4.5	Y	Y	Y
NBD	2.5	5	Y	Y	Y
NBD	2.5	5.5	Y	Y	Y
NBD	3	3	Y	Y	Y
NBD	3	4	Y	Y	Y
NBD	3	5	Y	Y	Y
NBD	3	5.5	Y	Y	Y
TDD	3	3	Y	Y	Y
TDD	3	4	Y	Y	Y
TDD	3	5	Y	Y	Y
TDD	3	5.5	Y	Y	Y
NBD + bag	3	3	Y	Y	Y
NBD + bag	3	4	Y	Y	Y
NBD + bag	3	5	Y	Y	Y
NBD + bag	3	5.5	Y	Y	Y
LPD2	3	3	Y	Y	Y
LPD2	3	4	Y	Y	Y
LPD2	3	5	Y	Y	Y
LPD2	3	5.5	Y	Y	Y
TDD + bag	3	3	Y	Y	Y
TDD + bag	3	4	Y	Y	Y
TDD + bag	3	5	Y	Y	Y
TDD + bag	3	5.5	Y	Y	Y
LPD2 + bag	3	3	Y	Y	Y
LPD2 + bag	3	4	Y	Y	Y
LPD2 + bag	3	5	Y	Y	Y
LPD2 + bag	3	5.5	Y	Y	Y
LPD1 + bag	3	3	Y	Y	Y
LPD1 + bag	3	4	Y	Y	Y
LPD1 + bag	3	5	Y	Y	Y
LPD1 + bag	3	5.5	Y	Y	Y
LPD1	3	3	Y	Y	Y
LPD1	3	4	Y	Y	Y
LPD1	3	5	Y	Y	Y
LPD1	3	5.5	Y	Y	Y
TDD	3	5	N	N	N
TDD	2.5	5	N	N	Y
LPD2	2.5	5	N	N	Y
NBD	2.5	5	N	N	Y
LPD1	2.5	5	N	N	Y
TDD + NBD	2.5	3, 3.5, 4, 5	N	N	N

Table 2. Summary of Flow Simulation settings

Simulation setting	Details
Computational domain	4 meters in front and 6 meters behind the dredge point of contact with the bottom. 2.8 to -0.2 meters from the bottom boundary (domain extended into the bottom). 2D-slice passed between struts.
Mesh	600 cells long by 180 cells high
Time setting	Time dependent 4 seconds with 1/24 second intervals
Boundary conditions	Bottom as ideal wall*

* Real wall was tested with no notable changes to simulation output

Table 3. Definitions of flow parameters examined in this study

Parameter	Details
Turbulent energy	Energy per unit mass of fluid associated with turbulent eddies (unit = J/kg)
Relative pressure	Force per unit area in the fluid and on the dredge frame relative to the background pressure (unit = Pa)

Table 4. Summary of particle study settings

Study setting	Details
Scaled scallop shell behavior behind NBD vs TDD	
Particle	Polystyrene sphere with a 100-cm diameter
Injections	2 cm below and 0.1, 0.2, 0.3, 0.5, and 1 meter behind the cutting bar
Bale angles	6.3 degrees for the NBD and 3 degrees for the TDD
LPD variants vs NBD and TDD	
Large particle	Polystyrene sphere with a 100-cm diameter
Small particle	Polystyrene sphere with a 25-cm diameter
Injections	2 cm, 5 cm, and 10 cm off the bottom in front of the cutting bar
Bale angles	All 5 degrees

Table 5. Results from flume tank tests (when measurements were taken). Highlighted values were used for CFD simulations.

Test #	Dredge	Speed	Model Tension (kg)	Warp Tension (lbs)	Bale angle (degrees)	Angle for plots	Scope Ratio
1	NBD no bag	2.5	2.183	1040	-2.5	-2.5	2.5
2	NBD no bag	3	2.438	1161	-2.5	-2.5	2.5
3	NBD no bag	3.5	2.821	1344	-2.5	-2.5	2.5
4	NBD no bag	4	3.396	1617	-0.6 to -1.3	-0.95	2.5
5	NBD no bag	4.5	3.984	1897	0.5	0.5	2.5
6	NBD no bag	5	4.658	2219	2.1	2.1	2.5
7	NBD no bag	5.5	5.203	2478	5.5	5.5	2.5
8	NBD no bag	3	2.452	1168	-2.5	-2.5	3
9	NBD no bag	4	3.294	1569	-2.5	-2.5	3
10	NBD no bag	5	4.48	2134	1.3 to 1.9	1.6	3
11	NBD no bag	5.5	5.081	2420	3.5	3.5	3
12	TDD no bag	3	2.615	1245	-1.6	-1.6	3
13	TDD no bag	4	3.452	1644	-1.6	-1.6	3
14	TDD no bag	5	4.565	2174	-1.6	-1.6	3
15	TDD no bag	5.5	5.22	2486	0.6 to 1.2	0.9	3
16	NBD w bag	3	5.203	2478	3.3	3.3	3
17	NBD w bag	4	6.85	3263	1.8	1.8	3
18	NBD w bag	5	8.303	3955	4.8	4.8	3
19	NBD w bag	5.5	9.063	4317	6.1	6.1	3
20	LPD v2 no bag	3	2.827	1346	-2.7	-2.7	3
21	LPD v2 no bag	4	3.478	1657	-2.7	-2.7	3
22	LPD v2 no bag	5	4.475	2131	1.7	1.7	3
23	LPD v2 no bag	5.5	4.965	2365	3.1	3.1	3
24	TDD w bag	3	5.808	2766	1.9	1.9	3
25	TDD w bag	4	6.918	3295	1.0	1.0	3
26	TDD w bag	5	8.117	3866	4.0	4.0	3
27	TDD w bag	5.5	8.795	4189	5.5	5.5	3
28	LPD v2 w bag	3	5.903	2811	2.7	2.7	3
29	LPD v2 w bag	4	7.038	3352	4.5	4.5	3
30	LPD v2 w bag	5	8.427	4014	4.2	4.2	3
31	LPD v2 w bag	5.5	9.209	4386	6.2	6.2	3
32	LPD v1 w bag	3	5.962	2840	2.7	2.7	3
33	LPD v1 w bag	4	6.835	3255	4.1	4.1	3
34	LPD v1 w bag	5	7.889	3757	3.6	3.6	3
35	LPD v1 w bag	5.5	8.656	4123	5.2	5.2	3
36	LPD v1 no bag	3	2.313	1102	-2.7	-2.7	3
37	LPD v1 no bag	4	2.896	1379	-2.7	-2.7	3
38	LPD v1 no bag	5	3.65	1738	1.4	1.4	3
39	LPD v1 no bag	5.5	4.144	1974	2.1	2.1	3
40	TDD no bag (dye)	5			3.0		2.5
41	LPD v2 no bag (dye)	5			1.0		2.5
42	NBD no bag (dye)	5			6.3		2.5
43	LPD v1 no bag (dye)	5			-0.6		2.5

Table 6. X-Y coordinates of marks on the wires during testing. Coordinates were used to plot catenary shapes.

Test #	Dredge_speed_warp	Mark	1	2	3	4	5	6	7	8	9
1	NBD no bag_2.5_2.5	x (mm)	0	976	1952	2899	3855	4800	5733		
		y (mm)	38	243	492	763	1075	1414	1781		
		y-adjusted	0	205	454	725	1037	1376	1743		
2	NBD no bag_3_2.5	x (mm)	0	968	1942	2876	3833	4762		5699	
		y (mm)	43	285	565	871	1198	1550		1916	
		y-adjusted	0	242	522	828	1155	1507		1873	
3	NBD no bag_3.5_2.5	x (mm)	0	961	1917	2856	3807	4733			
		y (mm)	43	329	639	965	1303	1672			
		y-adjusted	0	286	596	922	1260	1629			
4	NBD no bag_4_2.5	x (mm)	0	943	1889	2814	3774	4698			
		y (mm)	53	383	721	1070	1408	1777			
		y-adjusted	0	330	668	1017	1355	1724			
5	NBD no bag_4.5_2.5	x (mm)	0	939	1879	2804	3741	4669			
		y (mm)	69	420	767	1131	1500	1881			
		y-adjusted	0	351	698	1062	1431	1812			
6	NBD no bag_5_2.5	x (mm)	0	935	1870	2790	3734	4658			
		y (mm)	84	448	819	1197	1565	1939			
		y-adjusted	0	364	735	1113	1481	1855			
7	NBD no bag_5.5_2.5	x (mm)	0	927	1860	2778	3720	4646			
		y (mm)	121	494	863	1242	1604	1989			
		y-adjusted	0	373	742	1121	1483	1868			
8	NBD no bag_3_3	x (mm)	0	998	1988	2954	3940	4902	5883	6816	7794
		y (mm)	38	155	307	505	734	970	1243	1548	1863
		y-adjusted	0	117	269	467	696	932	1205	1510	1825
9	NBD no bag_4_3	x (mm)	0	988	1959	2936	3893	4863	5809	6767	
		y (mm)	36	240	460	704	967	1250	1536	1842	
		y-adjusted	0	204	424	668	931	1214	1500	1806	
10	NBD no bag_5_3	x (mm)	0	978	1942	2900	3854	4817	5760		
		y (mm)	52	308	575	861	1144	1440	1743		
		y-adjusted	0	256	523	809	1092	1388	1691		
11	NBD no bag_5.5_3	x (mm)	0	970	1931	2886	3840	4796	5741		
		y (mm)	59	342	620	914	1206	1517	1819		
		y-adjusted	0	283	561	855	1147	1458	1760		
12	TDD no bag_3_3	x (mm)	0	1000	1971	2974	3951	4912		6821	7766
		y (mm)	40	177	356	538	761	1018		1601	1930
		y-adjusted	0	137	316	498	721	978		1561	1890
13	TDD no bag_4_3	x (mm)	0	986	1960	2932	3885	4856	5798	6766	
		y (mm)	39	252	478	721	1001	1261	1564	1866	

		y-adjusted	0	213	439	682	962	1222	1525	1827	
14	TDD no bag_5_3	x (mm)	0	970	1928	2889	3843	4802	5748		
		y (mm)	48	313	586	870	1163	1460	1762		
		y-adjusted	0	265	538	822	1115	1412	1714		
15	TDD no bag_5.5_3	x (mm)	0	966	1923	2882	3831	4793	5738		
		y (mm)	57	342	633	918	1223	1523	1832		
		y-adjusted	0	285	576	861	1166	1466	1775		
16	NBD w bag_3_3	x (mm)	0	976	1940	2901	3860	4826	5768		
		y (mm)	60	307	563	832	1108	1396	1705		
		y-adjusted	0	247	503	772	1048	1336	1645		
17	NBD w bag_4_3	x (mm)	0	968	1930	2891	3845	4806	5750		
		y (mm)	72	355	627	908	1201	1499	1803		
		y-adjusted	0	283	555	836	1129	1427	1731		
18	NBD w bag_5_3	x (mm)	0	965	1921	2875	3829	4785	5728		
		y (mm)	107	398	693	993	1290	1593	1908		
		y-adjusted	0	291	586	886	1183	1486	1801		
19	NBD w bag_5.5_3	x (mm)	0	964	1919	2874	3822	4782	5725		
		y (mm)	123	421	720	1022	1331	1642	1947		
		y-adjusted	0	298	597	899	1208	1519	1824		
20	LPD v2 no bag_3_3	x (mm)	0	997		2958		4899		6814	7759
		y (mm)	35	187		577		1067		1651	1973
		y-adjusted	0	152		542		1032		1616	1938
21	LPD v2 no bag_4_3	x (mm)	0	991	1960	2930	3889	4855	5804	6765	
		y (mm)	38	244	477	728	991	1267	1562	1876	
		y-adjusted	0	206	439	690	953	1229	1524	1838	
22	LPD v2 no bag_5_3	x (mm)	0	978	1938	2893	3845	4812	5757		
		y (mm)	53	317	590	886	1184	1472	1767		
		y-adjusted	0	264	537	833	1131	1419	1714		
23	LPD v2 no bag_5.5_3	x (mm)	0	969	1929	2884	3839	4799	5746		
		y (mm)	60	339	628	921	1212	1510	1821		
		y-adjusted	0	279	568	861	1152	1450	1761		
24	TDD w bag_3_3	x (mm)	0	977	1943	2908	3859	4822	5769		
		y (mm)	54	307	568	835	1124	1418	1713		
		y-adjusted	0	253	514	781	1070	1364	1659		
25	TDD w bag_4_3	x (mm)	0	970	1930	2888	3841	4801	5747		
		y (mm)	82	353	633	918	1205	1519	1811		
		y-adjusted	0	271	551	836	1123	1437	1729		
26	TDD w bag_5_3	x (mm)	0	970	1923	2882	3833	4793	5737		
		y (mm)	110	399	692	983	1287	1600	1901		
		y-adjusted	0	289	582	873	1177	1490	1791		

27	TDD w bag_5.5_3	x (mm)	0	964	1919	2873	3824	4782	5726		
		y (mm)	124	428	719	1029	1334	1645	1957		
		y-adjusted	0	304	595	905	1210	1521	1833		
28	LPD v2 w bag_3_3	x (mm)	0	978	1942	2907	3862	4824	5771		
		y (mm)	60	314	575	846	1131	1425	1727		
		y-adjusted	0	254	515	786	1071	1365	1667		
29	LPD v2 w bag_4_3	x (mm)	0	970	1930	2890	3843	4805	5747		
		y (mm)	77	352	627	920	1212	1514	1820		
		y-adjusted		275	550	843	1135	1437	1743		
30	LPD v2 w bag_5_3	x (mm)	0	965	1919	2877	3828	4783	5732		
		y (mm)	113	400	692	988	1294	1608	1910		
		y-adjusted	0	287	579	875	1181	1495	1797		
31	LPD v2 w bag_5.5_3	x (mm)	0	966	1918	2874	3825	4780	5723		
		y (mm)	131	427	723	1029	1330	1646	1957		
		y-adjusted	0	296	592	898	1199	1515	1826		
32	LPD v1 w bag_3_3	x (mm)	0	977	1943	2907	3864	4825	5774		
		y (mm)	58	312	575	848	1129	1425	1719		
		y-adjusted	0	254	517	790	1071	1367	1661		
33	LPD v1 w bag_4_3	x (mm)	0	974	1934	2895	3846	4809	5751		
		y (mm)	72	347	628	908	1205	1503	1810		
		y-adjusted	0	275	556	836	1133	1431	1738		
34	LPD v1 w bag_5_3	x (mm)	0	970	1923	2878	3827	4788	5731		
		y (mm)	102	395	689	987	1293	1598	1904		
		y-adjusted	0	293	587	885	1191	1496	1802		
35	LPD v1 w bag_5.5_3	x (mm)	0	965	1918	2873	3826	4783	5733		
		y (mm)	121	416	720	1018	1320	1636	1933		
		y-adjusted	0	295	599	897	1199	1515	1812		
36	LPD v1 no bag_3_3	x (mm)	0	994	1982	2964	3944	4914	5884	6836	7800
		y (mm)	41	128	258	417	642	887	1125	1423	1760
		y-adjusted	0	87	217	376	601	846	1084	1382	1719
37	LPD v1 no bag_4_3	x (mm)	0	1004	1980	2950	3909	4878	5822	6785	
		y (mm)	44	218	424	651	906	1183	1472	1776	
		y-adjusted	0	174	380	607	862	1139	1428	1732	
38	LPD v1 no bag_5_3	x (mm)	0	986	1942	2906	3859	4823	5769		
		y (mm)	47	300	568	836	1110	1413	1714		
		y-adjusted	0	253	521	789	1063	1366	1667		
39	LPD v1 no bag_5.5_3	x (mm)	0	976	1926	2887	3843	4803	5744		
		y (mm)	57	337	622	910	1193	1494	1810		
		y-adjusted	0	280	565	853	1136	1437	1753		